DOI: http://dx.doi.org/10.1590/2179-10742018v17i11121

Microstrip Hybrid Coupler with a Wide Stop-Band Using Symmetric Structure for Wireless Applications

A. Rezaei[1] and L. Noori[2]
[1]Department of Electrical Engineering, Kermanshah University of Technology, Kermanshah, Iran
[2] Young Researchers and Elite Club, Kermanshah Branch, Islamic Azad University, Kermanshah, Iran
Email: Leila_noori62@yahoo.com

***Abstract*— In this paper, a wide stop-band microstrip coupler is presented. The proposed structure consists of coupled lines and step impedance cells, which are integrated to operate at 2.82 GHz for wireless applications. This coupler is formed by a symmetric structure so that the locations of the output ports relative to input are quite similar. Accordingly, the magnitudes (also phases) of S_{21} and S_{31} overlap each other so that input signal can be selected through the output ports equally. There are little differences between the magnitudes and phases of S_{21} and S_{31} so that 0.97° phase shift is obtained. In comparison with previous works, the performance of the introduced coupler is improved. To get a better isolation, return loss and harmonic attenuation the frequency response is optimized without significant increase in circuit size. Moreover, the first, second and third harmonics of S_{21} and S_{31} are well attenuated as well as a wide stop-band is obtained up to 15.1 GHz. The realized coupler is fabricated and measured. There is a good agreement between simulated and measured results, which confirms the design process.**

***Index Terms*—** Microstrip, coupler, isolation, wide stop-band, return loss.

I. INTRODUCTION

Hybrid couplers are important RF waveguide equipment in modern wireless communication systems. Generally, a RF coupler separates desired radio frequencies and transmits them through two output ports. This means that the harmonic elimination is a crucial issue. Microstrip couplers are favorite devices due to their low cost, planar structure and easy to integrate. According to these, many RF couplers have been introduced using various microstrip structures [1-14]. In [1] and [2] two compact microstrip branch line couplers have been designed for operating in 2.4 GHz and 5.7 GHz WLANs, respectively. Both of them consist of compact closed loops, step impedance cells, low impedance and high impedance sections. However, their frequency selections above and below passbands have not been well performed as well as harmonics have not been attenuated adequately. Due to the importance of harmonic attenuation, a harmonic suppression branch line coupler has been realized using a stub loaded close loop in [3]. In [4-6] dual-band branch-line couplers have been presented for multi-band communication systems. Stepped-impedance-stub lines [4], various stub loaded loops [5] and composite right/left-handed transmission lines [6] have been utilized to improve the dual-band

Brazilian Microwave and Optoelectronics Society-SBMO *received 29 Sep 2017; for review 5 Oct 2017; accepted 7 Dec 2017*
Brazilian Society of Electromagnetism-SBMag

ISSN 2179-1074

DOI: http://dx.doi.org/10.1590/2179-10742018v17i11121

performance. In [7] multi-rings resonators that occupy large area, have been employed to obtain two branch line couplers, which they cannot carry out any harmonic attenuation. A compact branch line coupler consisting of a ring resonator loaded by radial cells has been designed in [8] to attenuate the harmonics. Nevertheless, it does not perform the frequency selection suitably below the passband. In [9] four complex stubs have been loaded inside a closed quadrangular to miniaturize a coupler structure. The stubs are close together and fill the quadrangular space resulting in a complicated structure and hard fabrication. In [10] two ring resonators have been integrated to obtain three large microstrip branch line couplers with low performances where undesired coupling factor, isolation, return loss and insertion loss can be seen clearly. In [11] wide passband microstrip branch-line couplers have been designed by cascading several quadrangular loops, which take large implementation area. A microstrip coupler with large circuit size, undesired insertion loss and large phase shift has been offered in [12]. In [13] symmetrically and asymmetrically modified microstrip couplers have been proposed to operate in ISM 0.433 GHz. Although, they have been miniaturized correctly there are inappropriate insertion losses, coupling factors and phase shifts. Meanwhile, the frequency selection has not been done reasonably. The microstrip coupler reported in [14] has been miniaturized by substituting the quarter wave transmission lines in a conventional 90˚ coupler. The designed couplers in [10-14] could not attenuate the harmonics properly.

In this paper, a microstrip coupler with wide stop-band is designed for wireless applications. Several transmission zeros are created to improve the frequency selectivity and stop-band specifications. Due to its symmetric structure, the phases and amplitudes of S_{21} and S_{31} are balanced so that there are 0.97˚ phase shift and 0.5 dB amplitude shift. In addition, the performance of suggested coupler is good. The proposed structure is studied to find a method for tuning the resonance frequency.

II. DESIGNING METHOD

Fig.1a illustrates two similar resonators that are integrated in a same input port. The vertical coupled lines have been held in common between two resonators. The resonators are two open loops, which are marked in Fig.1a as Resonator1 and Resonator2. The step impedance structure helps to control the performance without size increment. In order to study the proposed structure an equivalent circuit is presented in Fig.1b where the effect of coupling is presented by the voltages V_{21} and V_{43}.

received 29 Sep 2017; for review 5 Oct 2017; accepted 7 Dec 2017

ISSN 2179-1074

DOI: http://dx.doi.org/10.1590/2179-10742018v17i11121

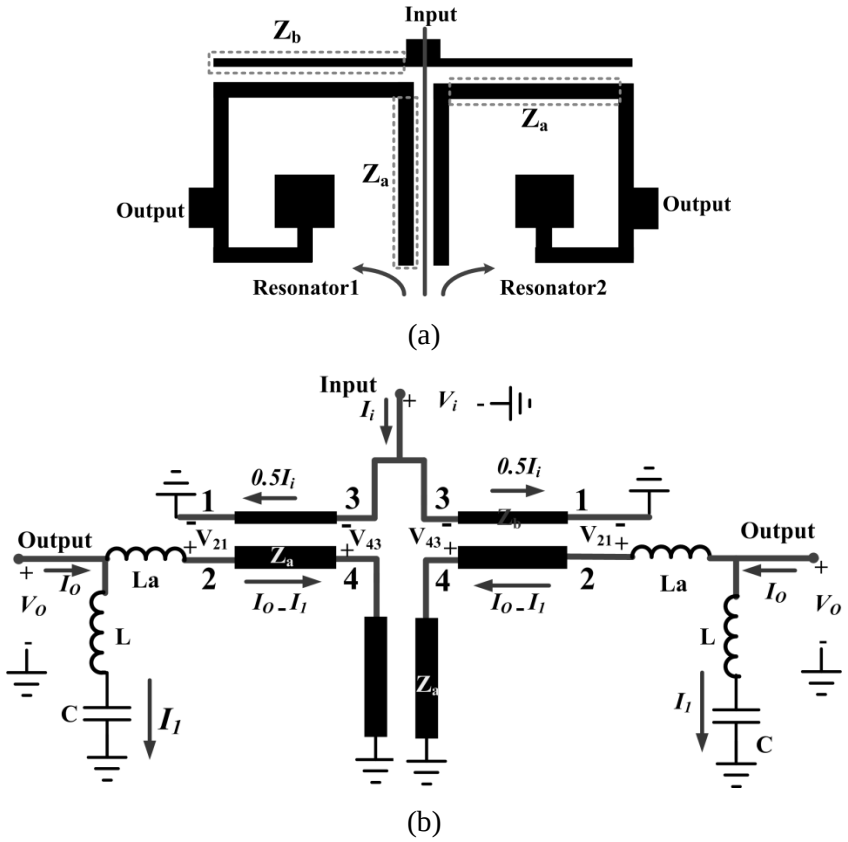

Fig.1. Proposed resonators (a) layout, (b) equivalent model.

Moreover, I_i, V_i, I_o and V_o are the input current, input voltage, output current and output voltage respectively. Since the effects of bents and step-in-widths are significant at higher than 10 GHz frequencies we ignore them. By this approximation, the step impedance structure connected to output port is modeled by a capacitor C (related to the wider part) and an inductor L. The inductor La is the effect of that line which incorporates horizontal coupled line and output port.

According to the equivalent circuit of the proposed structure the output voltage V_o and current I_1 are calculated as follows:

$$V_o = (j\omega La + 2Z_a)(I_o - I_1) = (jL\omega + \frac{1}{j\omega C})I_1 \Rightarrow I_1 = I_o(\frac{j\omega La + 2Z_a}{j\omega La + 2Z_a + jL\omega + \frac{1}{j\omega C}}) \quad (1)$$

where ω is the angular frequency. By substituting I1 from Equation (1) and knowing that $V_i=0.5I_iZ_b$, the output-input voltage ratio is calculated as follows:

$$\frac{V_o}{V_i} = \frac{I_o}{0.5I_i Z_b}(\frac{j\omega La + 2Z_a}{j\omega La + 2Z_a + jL\omega + \frac{1}{j\omega C}})(jL\omega + \frac{1}{j\omega C}) \quad (2)$$

In order to excite the resonators both resonators may be short circuits. Under this condition, $I_o = -0.5I_i$ and $V_o=V_i$ so that Equation (2) is simplified as follows:

received 29 Sep 2017; for review 5 Oct 2017; accepted 7 Dec 2017

ISSN 2179-1074

DOI: http://dx.doi.org/10.1590/2179-10742018v17i11121

$$(j\omega_r La + 2Z_a)(jL\omega_r + \frac{1}{j\omega_r C}) + Z_b(j\omega_r La + 2Z_a + jL\omega_r + \frac{1}{j\omega_r C}) = 0 \quad (3)$$

where ω_r is the angular resonance frequency. The last equation defines the relationship between the parameters at the resonance frequency. Therefore, we can tune the resonance frequency by changing inductors, capacitor and couple line structures based on Equation (3). The impedances Z_a and Z_b are depend on the electrical lengths of coupled lines, propagation constant and characteristic impedances of the transmission lines so that they can be defined as follows:

$$Z_a = jZ_{ca}\tan(\frac{\pi l f_r\sqrt{\varepsilon_{re1}}}{150})$$
$$Z_b = jZ_{cb}\tan(\frac{\pi l f_r\sqrt{\varepsilon_{re2}}}{150}) \quad (4)$$

where f_r is the resonance frequency in GHz, l is the length of coupled lines in mm, Z_{ca} and Z_{cb} are the characteristic impedances of the transmission lines and εre1 and ε_{re2} are the effective dielectric constants. The characteristic impedances and effective dielectric constants are depending on the width of lines [15]. However, for a little difference of widths we can assume that $\varepsilon_{re1}= \varepsilon_{re2}= \varepsilon_{re}$ and $Z_{ca}=Z_{cb}= Z_c$ resulting in $Z_a=Z_b$. From Equation (3), there is a high degree of freedom in selecting the parameters. For example, we can choose the resonance frequency at 2.8 GHz, l=10 mm, Z_c=50 Ω, $\varepsilon_{re1}= \varepsilon_{re2}$=1.7 as defaults then ω_r=5.6 π and $Z_a=Z_b$~j50. By substituting these values in Equation (3), we can select L_a, L and C. According to this method and using the proposed resonators, a microstrip coupler is designed. The layout of the proposed coupler is depicted in Fig.2. The corresponding dimensions are presented in Fig.2 in mm. In order to create the isolation port a similar structure is coupled to the analyzed structure. Additional optimization is carried out to improve the performance. For an example T-shape tapped line feed structures, are added to improve the coupling factor and insertion loss.

received 29 Sep 2017; for review 5 Oct 2017; accepted 7 Dec 2017

ISSN 2179-1074

DOI: http://dx.doi.org/10.1590/2179-10742018v17i11121

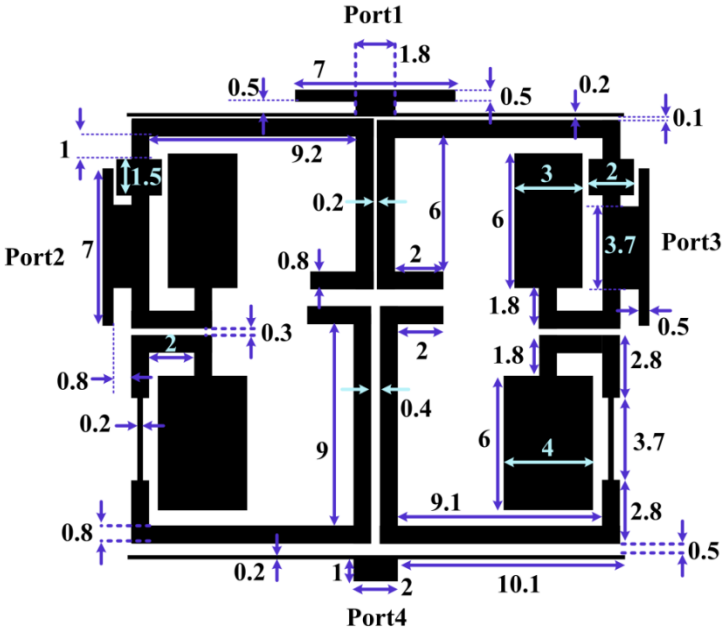

Fig.2. Layout configuration of the proposed coupler.

III. SIMULATION AND MEASURMENT RESULTS

The introduced coupler is designed to operate at 2.88 GHz and simulated using the ADS full wave EM simulator, then implemented on a RT Duroid 5880 substrate with a 2.22 dielectric constant, 31 mil-thickness and 0.0009 loss tangent. Finally, it was measured by an Agilent network analyzer N5230A. The proposed coupler has an overall size of $0.29\lambda g \times 0.26\lambda g$ (24.4mm × 29.1mm), where λg is the guided wavelength. The wide-band simulated frequency response consisting of S_{21}, S_{31}, S_{41} and S_{11} are demonstrated in Fig.3a. Due to the same positions of the output ports relative to the input port S_{21} is quite similar to S_{31}. Obviously, the wide stop bands with a minimum attenuation of -16.37 dB up to 7 GHz for both S_{21} and S_{31} are obtained. In order to better visibility, a narrow band frequency response is illustrated in Fig.3b. According to the achieved data, the insertion loss (S_{21}) and coupling factor (S_{31}) are 3.3 dB and 2.8 dB, respectively. Fig.3c depicts the measured and simulated return loss and isolation factor where they are 29.5 dB and 31.3 dB at the resonance frequency, respectively. The phase of S_{21} and S_{31} are shown in Fig.3d and the measured S_{21} and S_{31} are presented in Fig.3e. At the resonance frequency the phase of S_{21} and S_{31} are -114.75 and -113.78, respectively so that there is 0.97˚ phase difference between S_{21} and S_{31}. Because of the symmetrical structure, the phase of S_{21} and S_{31} are overlapped relatively. The phase difference between S_{21} and S_{31} is presented in Fig.3f. A photograph of the fabricated coupler is presented in Fig.3g

received 29 Sep 2017; for review 5 Oct 2017; accepted 7 Dec 2017

ISSN 2179-1074

DOI: http://dx.doi.org/10.1590/2179-10742018v17i11121

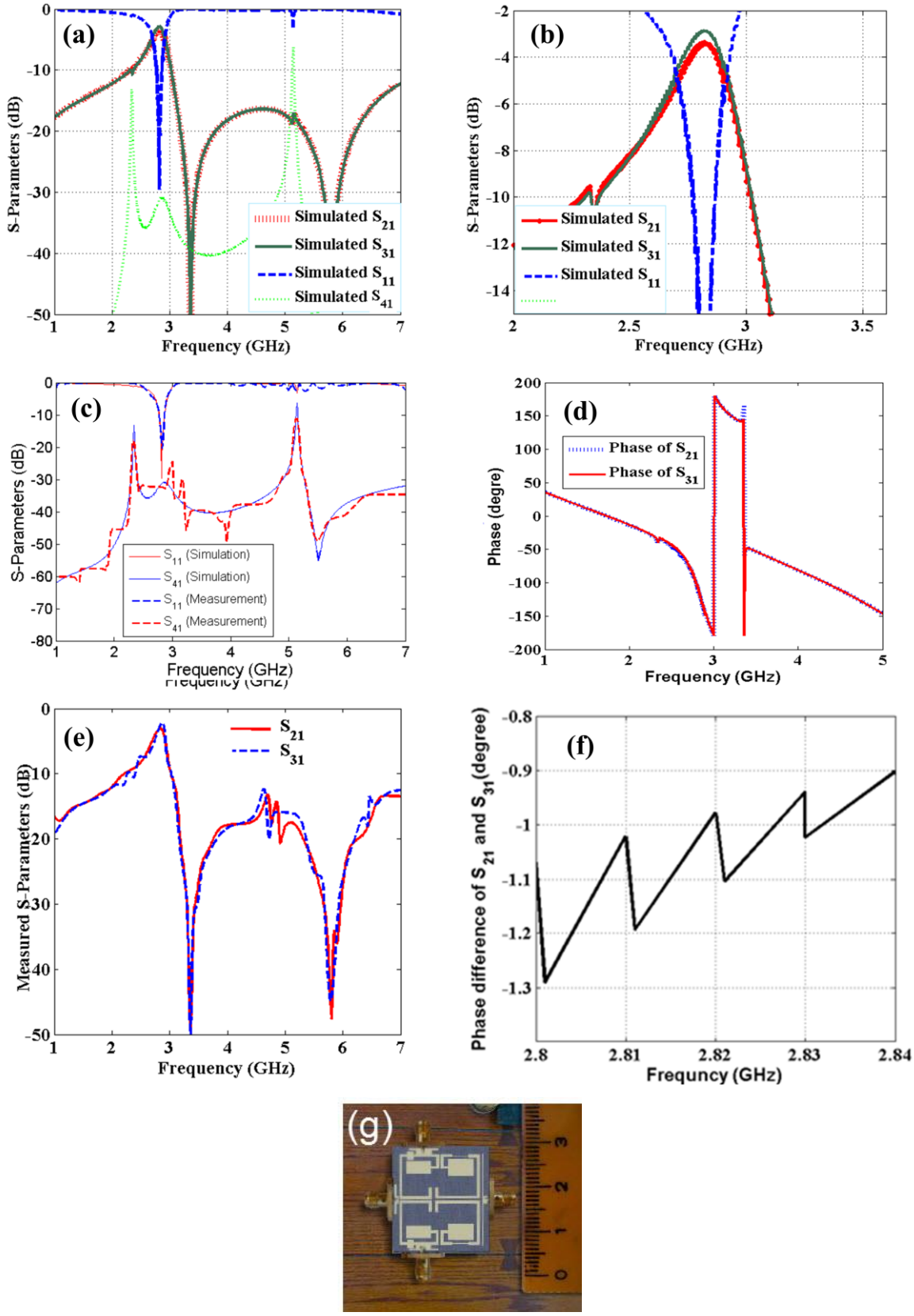

Fig.3. (a) Wide-band simulated return loss, isolation, insertion loss and the coupling factor, (b) narrow-band simulated return loss, insertion loss and the coupling factor, (c) simulated and measured return loss and isolation, (d) simulated phase of S_{21} and S_{31}, (e) measured frequency response, (f) phase difference of S_{21} and S_{31}, (g) a photograph of the fabricated structure.

received 29 Sep 2017; for review 5 Oct 2017; accepted 7 Dec 2017

ISSN 2179-1074

DOI: http://dx.doi.org/10.1590/2179-10742018v17i11121

The coupler performance and its size are compared with the previous works in Table I. It is clear that the realized coupler has relatively good performance and a compact structure. The obtained isolation is better than 90% of the referred papers in Table I while its return loss is better than all of them. Moreover, the obtained insertion loss and coupling factor only in [2] is better than our achievement. Phase shift less than 1˚ is achieved in [1, 2, 7] and the proposed coupler. Table II shows harmonics suppression in comparison with the previous works. In Table II, the highest attenuated harmonics are written for $|S_{21}| < 10\,dB$ and $|S_{31}| < 10\,dB$. In the proposed coupler and [3, 8] the first, second and third harmonics are attenuated. The first harmonics (magnitude of S_{21} and S_{31}) at 5.64 GHz ($2f_o$) are -28.7 dB, the second harmonics at 8.46 GHz ($3f_o$) are -13.68 dB and third harmonics at 11.28 GHz ($4f_o$) are -19.8 dB. Fig.4 demonstrates the harmonics of S_{21} and S_{31}. Above the passband S_{21} and S_{31} are attenuated up to 15.1 GHz with a minimum attenuation of -10 dB approximately.

According to the comparison Tables, the proposed coupler in [1] has better isolation and phase shift than our coupler. However, it has larger coupling factor and larger return loss without harmonic attenuation. Only the proposed diplexers in [3], [8] and this work could suppress the 4th harmonics. Nevertheless, our coupler has a better coupling factor, higher isolation and lower return loss than the designed couplers in [3] and [8]. Moreover, the introduced coupler in this work occupies smaller area and lower phase shift.

Table 1. Comparison of the proposed coupler and previous works (*Approximated Values)

References	S_{21} (dB)	S_{31} (dB)	S_{11} (dB)	S_{41} (dB)	Size (mm^2)	F_O (GHz)	Phase Shift
[1]	3.3	3.3	21.4	42.9	175.1	2.4	0.09 ˚
[2]	2.3	2.6	19.4	20.4	110	5.7	0.8 ˚
[3]	3.3	3.4	20.2	22.9	1361	1	1˚
[7]	3*	3*	20*	20*	1322	2	0˚
[8]	3.5	3.5	20	20	673	0.93	---
[9]	3.11	3.39	---	---	265.69	2	1 ˚
[10]	5	4	8	11	1553	3.5	10 ˚
[12]	7.3	2.25	29.33	21.5	819*	3	2.36˚
[13]	4.07	4.39	20.93	27.4	2218	0.433	2.14˚
[14]	---	3.3	20	24.2	204	1.07	1 ˚
This work	3.3	2.8	29.5	31.3	534.36	2.82	0.97

Table 2. Harmonics suppression in comparison with previous works (*Approximated Values)

References	2nd harmonic	3rd harmonic	4nd harmonic	Highest attenuated harmonic
[1]	No	No	No	No
[2]	No	No	No	No
[3]	Yes	Yes	Yes	7f$_o$
[7]	No	No	No	No
[8]	Yes	Yes	Yes	7.5fo
[9]	Yes	Yes	No	2.5f$_o$*
[10]	No	No	No	No
[11]	No	No	No	No
[12]	No	No	No	No
[13]	No	No	No	No
[14]	No	No	No	No
This work	Yes	Yes	Yes	5.24f$_o$

received 29 Sep 2017; for review 5 Oct 2017; accepted 7 Dec 2017

ISSN 2179-1074

DOI: http://dx.doi.org/10.1590/2179-10742018v17i11121

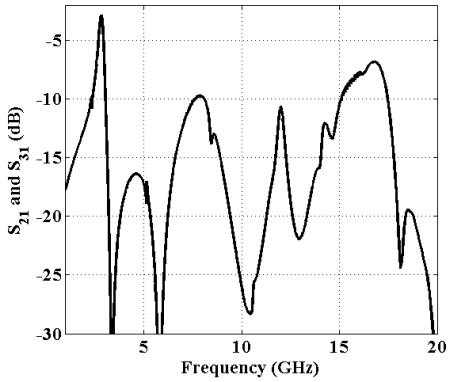

Fig.4. Harmonics of S_{21} and S_{31} up to 15.1 GHz.

IV. CONCLUSION

This paper presents a microstrip hybrid coupler operated at 2.82 GHz for wireless applications. The superiority of this coupler is creating a wide stop band up to 15.1 GHz where the first, second and third harmonics are attenuated properly. Moreover, there are several transmission zeros to improve the features of stop-band and selectivity. The phase curves of S_{21} and S_{31} depicts the phase shift of 0.97°. Furthermore, the designed coupler has not large dimensions while offers the isolation of -31.3 dB and return loss of -29.5 dB at the resonance frequency.

REFERENCES

[1] M. Salehi and L. Noori, "Novel 2.4GHz Branch-Line Coupler Using Microstrip Cells", Microwave and Optical Technology Letters, vol. 56, No.9, pp. 2110-2113, 2014.

[2] M. R. Salehi and L. Noori, "Novel Tunable Branch-Line Coupler for WLAN Applications", Microwave and Optical Technology Letters, Vol. 57, No. 5, pp.1081-1084, 2015.

[3] Y. Guo, L. B. Kang, W.G. Sheng, "Miniaturized Microstrip Branch-Line Coupler with Good Harmonic Suppression Performance", journal of electronics, Vol. 29, No.1, pp. 132-137, 2012.

[4] K. Chin, K. Lin, Y. Wei, T. Tseng, and Y. Yang, "Compact Dual-Band Branch-Line and Rat-Race Couplers with Stepped-Impedance-Stub Lines", IEEE Transaction on Microwave Theory and Techniques, Vol. 58, No. 5, pp. 1213 – 1221, 2010.

[5] M.J Park, and B. Lee, "Dual-Band Cross Coupled Branch Line Coupler", IEEE Microwave and Wireless Component Letters, Vol. 175, No. 10, pp. 655-657, 2005.

[6] Q. Wang, J. Lim and Y. Jeong, "Design of a compact dual-band branch line coupler using composite right/left-handed transmission lines", IET Electronic Letters, Vol. 52, No. 8, pp. 630–631, 2016.

[7] Y. Chun, and J. Hong. (2006). Compact Wide-Band Branch-Line Hybrids. IEEE Transaction on Microwave Theory and Techniques, 54(2), 704-709, 2006.

[8] A. Hazeri, A. Kashaninia, T. Faraji, M. Firouzi, "Miniaturization and Harmonic Suppression of the Branch-Line Coupler Based on Radial Stubs", IEICE Electronics Express, Vol. 8, No. 10, pp. 736-741, 2011.

[9] J. Wang, B. Wang, Y. Guo, L. Ong, S. Xiao, "A Compact Slow-Wave Microstrip Branch-Line Coupler with High Performance", IEEE Microwave and Wireless Component Letters, Vol. 17, No. 7, pp. 501-503, 2007.

received 29 Sep 2017; for review 5 Oct 2017; accepted 7 Dec 2017

ISSN 2179-1074

DOI: http://dx.doi.org/10.1590/2179-10742018v17i11121

[10] N.A. M. Shukor and N. Seman, "Enhanced Design of Two-Section Microstrip-Slot Branch Line Coupler with the Overlapped k/4 Open Circuited Lines at Ports", Springer Wireless Personal Communications, Vol. 88, No. 3, pp. 467-488, 2016.

[11] C-W. Tang, C-T. Tsengand K-C. Hsu, "Design of Wide Passband Microstrip Branch-Line Couplers with Multiple Sections", IEEE Transactions on Component, Packaging and Manufacturing Technology, Vol. 4, No.7, pp. 1222 – 1227, 2014.

[12] A. B. Santiko, Y. P. Saputera and Y. Wahyu, "Design and Implementation of Three Branch Line Coupler at 3.0 GHz Frequency for S-Band Radar System" The 22nd Asia-Pacific Conference on Communications, pp. 315-318, 2016.

[13] S. Velan and M. Kanagasabai, "Compact Microstrip Branch-Line Coupler with Wideband Quadrature Phase Balance", Microwave and Optical Technology Letters, Vol. 58, No. 6, pp. 1369-1374, 2016.

[14] S. Shamsinejad, M. Soleimani, N. Komjani, "Novel Enhanced and Miniaturized 90° Coupler for 3G EH Mixers", IEEE Microwave and Millimeter Wave Technology, pp. 1264 – 1267, 2008.

[15] J.-S. Hong and M.J Lancaster, "Microstrip Filters for RF/Microwave Applications", John Wiley & Sons, 2001.

received 29 Sep 2017; for review 5 Oct 2017; accepted 7 Dec 2017

ISSN 2179-1074